Available online at www.sciencedirect.com
ScienceDirect
Journal of Solid State Chemistry 181 (2008) 587–592
JOURNAL OF SOLID STATE CHEMISTRY
www.elsevier.com/locate/jssc

# Shape evolution and thermal stability of Ag nanoparticles on spherical $SiO_2$ substrates

Shaochun Tang, Shaopeng Zhu, Haiming Lu, Xiangkang Meng*

*National Laboratory of Solid State Microstructures, Department of Materials Science and Engineering, Nanjing University, Nanjing 210093, PR China*

Received 2 September 2007; received in revised form 20 December 2007; accepted 6 January 2008
Available online 12 January 2008

**Abstract**

In this paper, the shape evolution and thermal stability of Ag nanoparticles (NPs) on spherical $SiO_2$ substrates were investigated by means of *in situ* transmission electron microscopy (TEM) imaging and differential scanning calorimetry (DSC). The initial Ag NPs at room temperature were semispherical-like, with an average size of 9 nm in half-height width, well-dispersed on spherical $SiO_2$ substrates. No obvious shape change was observed when the semispherical NPs of Ag were heated at temperature lower than 550 °C. The shape of the semispherical Ag NPs changed gradually into a spherical one in the temperature range of 550–700 °C, where surface diffusion and surface premelting took place. When the heating temperature was increased up to 750 °C, the spherical Ag NPs were found to desquamate from the substrates due to the decreases of the contact area and the binding force between Ag NPs and $SiO_2$ substrates. A possible mechanism for the desquamation of Ag NPs from the $SiO_2$ sphere surface is proposed according to the results of *in situ* TEM observation and DSC analysis.


*Keywords:* Ag nanoparticles; $SiO_2$/Ag composite; *In situ* observation; Thermal stability

## 1. Introduction

Dielectric–metal core-shell building structure, such as $SiO_2$/metal composite consisting of spherical $SiO_2$ core and nanocoating of dispersive metal nanoparticles (NPs) shell, has found many potential applications in optical modulation [1,2], biological detection [3–5], antibacterial treatment [6], surface-enhanced Raman scattering [7], and so on. In general, these composite particles were fabricated by depositing metal NPs onto a $SiO_2$ sphere surface. The discrete metal NPs on the substrates usually have the advantages of well-dispersed distribution and controllable number density, which may have novel properties because of the strong correlation between properties of metal NPs and their organization [8]. In the synthesis process, metal particles usually interact with the $SiO_2$ surface in the form of chemical bonds (e.g., Si–O–Ag bonds) or relatively strong physical adhesion to create the effective bonding force [9–14]. However, this effective bonding force will be altered with the change of environmental temperature due to the temperature dependence of the surface groups on $SiO_2$ [15] and therefore influence the thermal stability of the composite particles. Besides, the physical and chemical properties of these metal NPs themselves are usually temperature-dependent [16–18]. Furthermore, material application has to be realized in some serving conditions, e.g., many applications would require heating the reaction system. Thus, it is of significance to investigate the thermal stability of $SiO_2$/metal composite particles for their property amelioration and applications.

It is well known that *in situ* observation is useful for the study of temperature-induced phase transformation, interfacial diffusion and structural evolution in order to understand the structure and structural stability of nanocomposite materials [19,20]. In the present work, *in situ* transmission electronic microscopy (TEM) imaging is first applied to study the shape evolution and thermal stability of Ag NPs on spherical $SiO_2$ substrates. The chamber of the transmission electron microscope provides a special environment

*Corresponding author. Fax: +86 25 8359 5535.
*E-mail address:* mengxk@nju.edu.cn (X. Meng).

0022-4596/$ - see front matter © 2008 Elsevier Inc. All rights reserved.
doi:10.1016/j.jssc.2008.01.014

where the effects of extrinsic factors (such as humidity, surface adsorbate, oxygen and so on) are eliminated. In this case, thermal stability of Ag NPs on spherical $SiO_2$ substrates is only affected by intrinsic factors such as the size, morphology and distribution of Ag NPs, and interfacial binding between Ag NPs and $SiO_2$ substrates.

Considering the particularity of this kind of $SiO_2$/Ag nanocomposite, several questions may be raised: (1) What is the temperature at which the surfaces of Ag NPs begin to premelt, i.e., the temperature at which liquid and solid Ag coexist? (2) Is there a temperature-induced shape evolution? (3) Which kind of shape does the final Ag NPs take, particle agglomerations, a consecutive film or isolated spherules? (4) Are the Ag NPs inclined to stay on the surface of the $SiO_2$ substrates or desquamate from them as the temperature increases? (5) Which will happen first, temperature-induced shape evolution or desquamation of the Ag NPs? (6) Does the size affect the thermal stability of Ag NPs in the $SiO_2$/Ag composite system? To answer these questions, we made real-time TEM observation and DSC analysis on the $SiO_2$/Ag nanocomposite.

## 2. Experimental details

After pre-preparation of monodisperse colloidal $SiO_2$ spheres using the modified StÖber method [21], Ag NPs were deposited onto the colloidal $SiO_2$ surface to fabricate $SiO_2$/Ag composite particles by our newly reported method of ultrasonic electrodeposition [12,13]. The Ag NPs with different sizes and different distribution uniformity on $SiO_2$ spheres were obtained by adjusting the reaction parameters of ultrasonic electrodeposition. The *in situ* TEM observation was conducted on a JEM-200CX transmission electronic microscope equipped with a heating sample holder. The vacuum inside the microscope was maintained at $1.0 \times 10^{-4}$ Pa. The $SiO_2$/Ag composite particles were dispersed on an ultrathin amorphous carbon film supported by standard Cu grids for heating in the microscope. The heating was started at room temperature, and ended at 800 °C, which was measured by a thermocouple mounted in the heater. The local temperature at the specimen region where the TEM was imaged is slightly different because of electron beam-heating effect. A temperature error of $\pm 15$ °C is estimated according to the laboratory reliability tests. Low electron intensity was chosen to prevent any uncontrolled changes during the temperature-rise period. Specimens annealed at different temperatures in the JEM-200CX microscope were further analyzed in a high-resolution FEI TECNAI F20 microscope. DSC (NETZSCH STA 449C-Thermal Star 300) analysis of the $SiO_2$/Ag composite particles was carried out up to a temperature of 800 °C at a heating rate of 10 °C/min under a flowing gas of nitrogen.

## 3. Results and discussion

Fig. 1 shows a series of TEM images of a $SiO_2$/Ag composite particle heated from room temperature to 750 °C. At room temperature (Fig. 1a), Ag NPs with a narrow size range are spotted homogeneously in the form of random blobs on the $SiO_2$ surface. As is well known that Ag NPs have low-temperature sintering behavior, for example, Ag NPs of ~20 nm exhibited obvious sintering behavior at a significantly lower temperature of ~150 °C [22]. However, the Ag NPs in the sample did not experience a coalescence when the sample was annealed at temperatures below 550 °C. In addition, the shape of most Ag NPs in the sample shows no obvious change (Figs. 1a–e). This may be attributed to the discrete characteristic of the Ag NPs and the large spaces between them [23]. When the annealing temperature was higher than 550 °C (Figs. 1e–f), the morphology of Ag NPs was observed to change gradually from semisphere into sphere with a smaller radius of curvature. The detailed reasons for this shape evolution will be discussed later. When heating temperature reaches 750 °C, the Ag NPs were observed to desquamate gradually from the $SiO_2$ sphere. Fig. 1g displays the almost bare $SiO_2$ substrate with only a few Ag NPs after heating at 750 °C. As shown in Fig. 1h, the desquamated Ag NPs are spherical with an average diameter of 9–12 nm and dispersed on the carbon film. Note that the sample is firstly annealed at 750 °C for 20 min in the JEM-200CX microscope and then imaged in the FEI TECNAI F20 microscope. Fig. 1i is a high-resolution transmission electron microscopy (HRTEM) image of one single desquamated Ag nanoparticle. It is a perfect single crystal with a size of 9 nm in diameter. The mechanism of the desquamating process will be discussed later in detail.

Two sets of samples were further observed by a TECNAI F20 microscope to show the shape evolution more clearly. One is the as-deposited $SiO_2$/Ag composite particles, and the other is the sample annealed at 650 °C for 20 min in the microscope. TEM images of the as-deposited

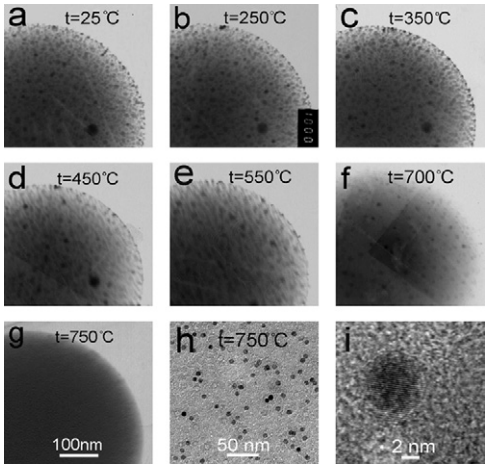


Fig. 1. (a)–(g) A series of *in situ*-recorded TEM images of a $SiO_2$/Ag composite particle heated from 25 to 750 °C, exhibiting shape evolution and desquamation process of Ag NPs from the surface of $SiO_2$ substrates with the increase of temperature. (h) TEM image of the Ag NPs desquamated from $SiO_2$ substrates and (i) HRTEM image of a single Ag nanoparticle in (i). The scale bar in (g) is the same with those of (a–f).

samples are shown at different magnifications in Figs. 2a–d. It can be seen that Ag NPs with sizes of 8–11 nm are dispersed homogeneously on the surface of the $SiO_2$ spheres (Figs. 2a and b). Here the size of Ag NPs is measured by the width at half their height. At higher magnification (Figs. 2c and d), the Ag NPs are observed to be hemispherical with rough surfaces. The average distance between the bottoms of two adjacent particles is 3 nm. TEM images of the annealed sample are shown at different magnifications in Figs. 2e–h. It is interesting to note that the morphology of the annealed Ag NPs on the $SiO_2$ sphere is spherical with smooth surfaces and the diameter is in the range of 9–12 nm. Moreover, the average space between two adjacent particles enlarges to 5 nm. It is obvious that the shape, size, distance and surface roughness of Ag NPs all changed after the sample was annealed at 650 °C. Instead of a coalescence or Ostwald ripening, the discrete Ag NPs in our experiments only experience shape evolution during the annealing process. It can also be confirmed by the fact that the volumes of the Ag NPs before and after annealing are approximately equivalent according to the approximate calculations (the average volume of the hemispheres and the spherical Ag NPs are calculated to be about 1133 $nm^3$ in Fig. 2c and 1149 $nm^3$ in Fig. 2g, respectively). In accordance with the *in situ* observation results mentioned above, this contrastive observation indicates the shape evolution of Ag NPs before their desquamation from the $SiO_2$ substrates.

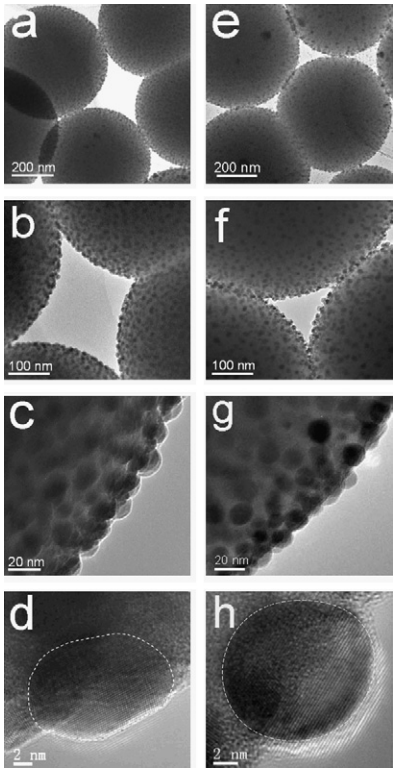


Fig. 2. A contrastive observation between the $SiO_2$/Ag composite particles at room temperature and those annealed at 650 °C. (a)–(d) TEM images with different magnifications of $SiO_2$/Ag composite particles at room temperature; (e)–(h) TEM images with different magnifications of $SiO_2$/Ag composite particles annealed at 650 °C. To highlight the shape evolution, dashed curves were portrayed along the boundaries of the NPs shown in (d) and (h), respectively.

Figs. 3a–d show SAED patterns of an entire $SiO_2$/Ag composite particle at 25, 250, 650, and 750 °C. Fig. 3a indicates that the Ag NPs on the $SiO_2$ surface are randomly oriented and the recognizable diffraction rings correspond to (111), (200), (220) and (311) faces of face-centered-cubic (fcc) structured Ag (JCPDS card No. 4-783), respectively. Compared with Fig. 3a, the intensity of electron diffractions of Figs. 3b and c gets stronger, indicating that the crystallinity of Ag NPs after annealing becomes higher. Except for the diffraction rings of (111), (200), (220) and (311) faces, the diffraction ring of the (331) face is also found in Fig. 3c, which indicates a higher crystallinity of the Ag NPs. At 750 °C, however, the recognizable diffraction rings of metallic Ag are missing and only few weak diffraction spots can be found, which may result from the residual small quantity of Ag NPs on $SiO_2$, as shown in Fig. 3d. This further confirms that most of the Ag NPs have desquamated from the $SiO_2$ spheres. The SAED analysis shows that the crystallinity of Ag NPs increases with the increase of temperature until they desquamate.

DCS analysis was used in order to assess the temperature-dependent behavior of Ag NPs in the composite particles. DCS curves of the uncoated StÖber's $SiO_2$ spheres and the $SiO_2$ spheres coated with Ag NPs are shown in Figs. 4a and b, respectively. In Fig. 4a, no obvious peak is observed except for an endothermic peak in the region of 50–70 °C, which is induced by the loss of adsorbed species and solvent molecules. In Fig. 4b, besides the peak of 50–70 °C, three endothermic peaks at about 350, 410 and 700 °C can also be observed. The peak at about 350 °C corresponds to the absorption of heat induced by the separation of surface groups on $SiO_2$, such as –OH and so on [11,15]. The peak at about 410 °C might be corresponding to the beginning of surface premelting of the Ag NPs, which eventually induced the shape evolution of the Ag NPs at about 650 °C, as is discussed above. The broad endothermic peak at about 700 °C might be attributed to the possible breaking of Si–O–Ag chemical bonds, where the Ag NPs gradually desquamate from the surface of $SiO_2$, as shown in Fig. 1f. As indicated by the

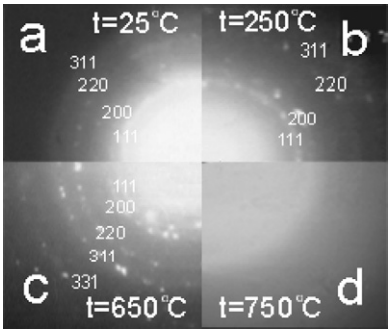


Fig. 3. SAED patterns of an entire $SiO_2$/Ag composite particle at (a) 25 °C, (b) 250 °C, (c) 650 °C and (d) 750 °C, respectively.

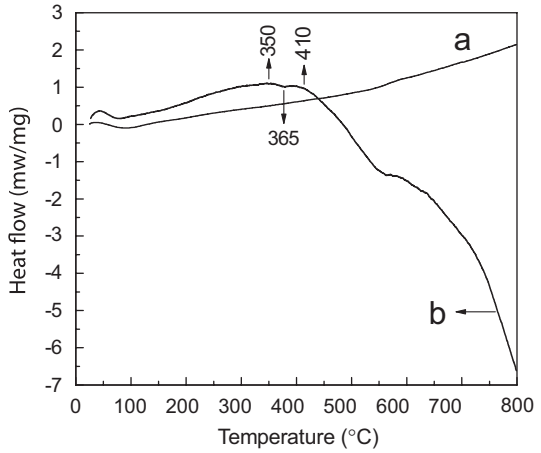


Fig. 4. DCS curves of uncoated StÖber's $SiO_2$ substrate (a) and $SiO_2$/Ag composite particles (b).

exothermic peak in the DSC spectrum, the amorphous-to-crystalline transition of the Ag NPs coated on $SiO_2$ occurred at about 365 °C, which is very close to 340 °C reported by Salkar et al. [24]. These temperature points are approximately consistent with the results of *in situ* TEM observation.

According to the above observations, the temperature-induced changes of $SiO_2$/Ag composite particles mainly contain two stages, i.e. the shape evolution and desquamation of Ag NPs. The former follows the rule of the minimizing tendency of the surface energy. The Ag NPs are inclined to take spherical shape to minimize their surface energy. With the increase of temperature, more surface atoms of Ag NPs in the thermal field are excited and their vibration become intense, which facilitates the process of minimizing the surface energy. Specifically, the process favorable to the shape evolution of Ag NPs includes two main aspects: (1) Surface diffusion. In the whole heating process, surface diffusion, which would lead to a three-dimensional atomic rearrangement [19], could be more apparent with the increase of temperature. (2) Surface premelting. Unlike surface diffusion, surface premelting of Ag NPs takes place beyond a certain temperature, and it induces the formation of a liquid layer covering the Ag solid. Because the liquid Ag and the amorphous solid $SiO_2$ substrate are totally nonwettable, surface tension compels this liquid layer to circle the solid Ag. As for the desquamation of Ag NPs, it is related to kinetics effect. In our case, the activation energy for desorption ($E_d$) of the supported Ag NPs can be defined as the energy needed for rupture of Si–O–Ag bonds and for physical desorption. The $E_d$ of the Ag NPs decreases with the decrease of contact area. And hence, according to the well-known Arrhenius equation ($k_d = k_0 \exp(-E_d/RT)$, where $K_0$ is a pre-exponent constant and $T$ is the annealing temperature), the desorption of Ag NPs from $SiO_2$ substrates is increasingly favored with the increase of annealing temperature. Thus, the desquamation of Ag NPs takes place when the temperature is increased to the extent that binding forces between Ag NPs and $SiO_2$ substrates are eliminated.

The detailed shape evolution and desquamation of Ag NPs are suggested as follows: at the first stage, Ag NPs are relatively firmly attached to $SiO_2$ substrates because of physical binding and chemical bonds (e.g., Si–O–Ag bonds). With the increase of temperature, surface atoms of Ag NPs are excited and surface diffusion intensifies in the promotion of surface premelting [19]. Beyond a certain temperature, surface premelting of Ag NPs takes place, and it induces the formation of a core-shell structure consisting of Ag solid and a liquid layer. Because the liquid Ag and the amorphous solid $SiO_2$ substrate are totally nonwettable, the interface tension $\gamma_{SL}$ between liquid Ag and $SiO_2$ points tangentially inwards, enabling the liquid layer to tightly cover solid Ag. As the temperature further increases, the solid Ag covered by the liquid layer continues melting, which decreases the contact area between solid Ag NP and $SiO_2$ at the continuous tangential interface tension. Note that the interface tension is the only tangential force exerted at the intersection points of three phases (liquid Ag, solid Ag and $SiO_2$). With the shrinkage of contact area, physical and chemical binding forces decrease gradually. The shrinkage gets more obvious until at 700 °C where the solid Ag is circled completely by a liquid layer. As a result, the particles become spherical in point-contact with $SiO_2$. Thus, the Ag NPs experience a shape evolution from semisphere to sphere with a smaller radius of curvature and a smoother surface in the temperature range of 550–700 °C (Figs. 1e and f). Then, the Ag NPs begin to slide off the surface of $SiO_2$ because of thermal disturbance and remain spherical. Finally, almost all the NPs fell off the substrates as single spherical NPs. According to the above-mentioned results, a simple sketch of the shape evolution and desquamation process of the Ag NPs from $SiO_2$ substrate is shown in Fig. 5.

It is well known that the thermal stability of metal NPs is strongly dependent on their size. $SiO_2$/Ag composite particles with Ag NPs of different sizes were used to investigate the size effect on thermal stability. Fig. 6 shows a series of representative TEM images of $SiO_2$/Ag composite particles heated from 25 to 800 °C. The average sizes of Ag NPs at room temperature shown in Fig. 6a are measured to be 25 nm. The SAED pattern of an entire $SiO_2$/Ag composite particle, as shown in the lower right corner of Fig. 6a, indicates that the Ag NPs are randomly oriented on the $SiO_2$ surface. The diffraction rings consisting of discontinuous diffraction spots respectively correspond to (111), (200) and (220) faces of fcc structured Ag (JCPDS No. 4-783). It is observed that the shape of Ag NPs shows no obvious change up to 650 °C (Figs. 6a–c). There is a shape evolution of the Ag NPs from semisphere to sphere in the temperature range of 650–750 °C (Figs. 6d and e). When the temperature is increased up to 800 °C (Fig. 6f), most Ag particles desquamated from the substrates, which is also confirmed by the SAED pattern

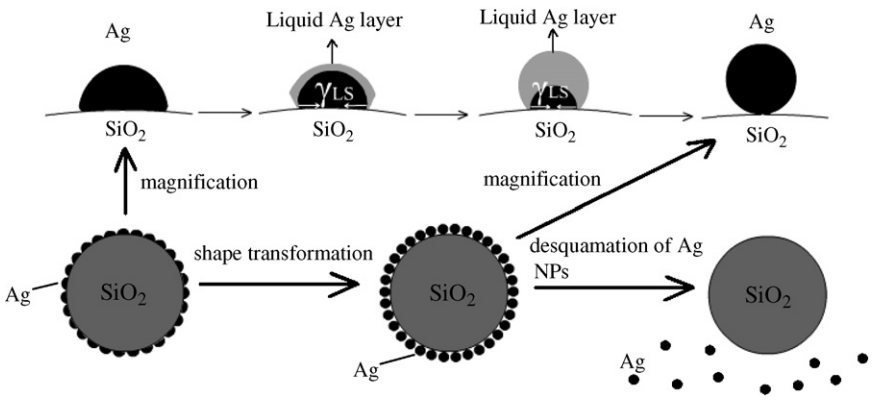


Fig. 5. A simple sketch for the shape evolution and desquamation process of the Ag NPs.

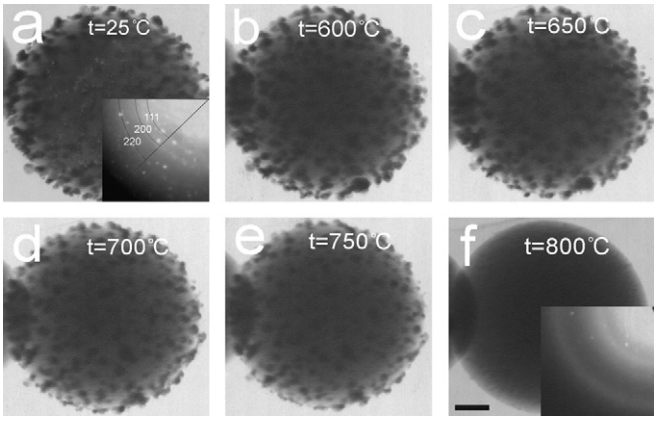


Fig. 6. A series of representative TEM images of a $SiO_2$/Ag composite particle heated from 25 to 800 °C. The scale bar in (f) is 100 nm, which is the same as those of (a–e).

(see the lower right corner of Fig. 6f). A similar shape evolution and desquamation process observed again confirms the temperature-dependent behavior of Ag NPs in the $SiO_2$/Ag composite system. These results indicate that the surface premelting temperature, shape evolution temperature and desquamation temperature all increase with the increase of the size of Ag NPs.

Consequently, the several above-mentioned questions can be explained as follows: (1) As for Ag NPs with average sizes of 9 and 25 nm in our study, surface premelting begins at 550 and 650 °C, respectively, much lower than the melting point of bulk metallic Ag (961 °C), which may originate from the surface tension of the colloid (solid–liquid) interface ($\gamma_{SL}$) [20]. (2) There is a temperature-induced shape evolution from hemisphere to sphere due to surface premelting and interface tension. (3) The final Ag particles, after they desquamate from the $SiO_2$ substrate, are isolated spherules. (4) As for the Ag NPs with an average size of 9 nm, there is a temperature-induced desquamation of Ag NPs at 700 °C. (5) The shape evolution happens before the desquamation of the Ag NPs. (6) The larger the initial sizes of the Ag NPs, the higher the corresponding characteristic evolution temperatures.

## 4. Conclusions

In summary, temperature-induced shape evolution and desquamation of Ag NPs (9 nm in half-height width) on spherical $SiO_2$ substrates were studied by *in situ* TEM observation. The shape of Ag NPs showed no obvious change up to 550 °C. It experienced an evolution from semisphere to sphere with smaller radius of curvature and smoother surface in the temperature range of 550–700 °C, where surface diffusion and surface premelting took place. When the temperature increased up to 750 °C, the spherical Ag NPs desquamated from the substrate. The size effect on the thermal stability of Ag NPs in the $SiO_2$/Ag composite system was also studied. A possible mechanism for the desquamation of Ag NPs from the $SiO_2$ sphere surface is proposed according to the *in situ* TEM observation and DSC analysis. This work signifies the thermal stability improvement of $SiO_2$/metal composite particles.

## Acknowledgments

This research was supported by a grant for the State Key Program for Basic Research of China (Grant no. 2004CB619305), the National Natural Science Foundation of China (Grant no. 50571044), the Natural Science Foundation of Jiangsu Province (Grant no. BK2006716), and the Postdoctoral Science Foundation of China (Grant no. 2007410326).

## References

[1] R.D. Averitt, S. Westcott, N.J. Halas, J. Opt. Soc. Am. 16 (1999) 1824.
[2] Y. Lu, Y. Yin, Z.Y. Li, Y. Xia, Nano Lett. 2 (2002) 785.
[3] C. Loo, A. Lowery, N. Halas, J. West, R. Drezek, Nano Lett. 5 (2005) 709.
[4] S.I. Stoeva, F.W. Huo, J.S. Lee, C.A. Mirkin, J. Am. Chem. Soc. 127 (2005) 15362.
[5] S. Phadtare, A. Kumar, V.P. Vinod, C. Dash, D.V. Palaskar, M. Rao, P.G. Shukla, S. Sivaram, M. Sastry, Chem. Mater. 15 (2003) 1944.
[6] Y.H. Kim, D.K. Lee, H.G. Cha, C.W. Kim, Y.S. Kang, J. Phys. Chem. C 111 (2007) 3629.
[7] S. Nie, S.R. Emory, Science 275 (1997) 1102.

[8] Y.H. Kim, D.K. Lee, H.G. Cha, C.W. Kim, Y.S. Kang, Chem. Mater. 19 (2007) 5049.
[9] T. Nakanishi, B. Ohtani, K. Uosaki, J. Phys. Chem. B 102 (1998) 1571.
[10] K. Hu, M. Brust, A.J. Bard, Chem. Mater. 10 (1998) 1160.
[11] V.G. Pol, D.N. Srivastava, O. Palchik, V. Palchik, M.A. Slifkin, A.M. Weiss, A. Gedanken, Langmuir 18 (2002) 3352.
[12] S.C. Tang, Y.F. Tang, F. Gao, Z.G. Liu, X.K. Meng, Nanotechnology 18 (2007) 295607.
[13] S.C. Tang, Y.F. Tang, S.P. Zhu, H.M. Lu, X.K. Meng, J. Solid State Chem. 180 (2007) 2871.
[14] Y.H. Kim, D.K. Lee, C.W. Kim, H.G. Cha, Y.S. Kang, B.G. Jo, J.H. Jeong, Mol. Cryst. Liq. Cryst. 464 (2007) 665.
[15] R.D. Badley, W.T. Ford, F.J. McEnroe, R.A. Assinks, Langmuir 6 (1990) 792.
[16] H.C. Kim, T.L. Alford, D.R. Allee, Appl. Phys. Lett. 81 (2002) 4287.
[17] R. Seemann, S. Herminghaus, K. Jacobs, Phys. Rev. Lett. 86 (2001) 5534.
[18] M.W. Zhu, G.D. Qian, Z.Y. Wang, M.Q. Wang, Mater. Chem. Phys. 100 (2006) 333.
[19] Z.L. Wang, Adv. Mater. 15 (2003) 1497.
[20] Z.L. Wang, J.M. Petroski, T.C. Green, M.A. El-Sayed, J. Phys. Chem. B 102 (1998) 6145.
[21] W. StÖber, A. Fink, E. Bohn, J. Colloid Interface Sci. 26 (1968) 62.
[22] K.S. Moon, H. Dong, R. Maric, S. Pothukuchi, A. Hunt, Y. Li, C.P. Wong, J. Electron. Mater. 34 (2005) 168.
[23] E. Sutter, P. Sutter, Y.M. Zhu, Nano Lett. 5 (2005) 2092.
[24] R.A. Salkar, P. Jeevanandam, T. Aruna, Y. Koltypin, A. Gedanken, J. Mater. Chem. 9 (1999) 1333.